Validity of the diffusion equation at the atomic scale investigated via numerical simulations

Y. Adda,[1] J. Philibert,[2] and V. Pontikis[3,*]

[1]*C2RMF-UMR 171 Palais du Louvre, 14, quai F. Mitterrand, 75 001 Paris, France*

[2]*24, rue Sainte Radegonde, 78100 Saint Germain-en-Laye, France*

[3]*Laboratoire des Solides Irradiés (LSI), Institut Rayonnement Matière de Saclay (IRAMIS), Commissariat à l'Energie Atomique (CEA), 91191 Gif-sur-Yvette Cedex, France*

(Received 17 October 2011; revised manuscript received 5 March 2012; published 30 April 2012)

In the absence of theoretical predictions or experimental determinations, numerical simulations are used for establishing the region over which diffusive mass fluxes linearly relate to concentration gradients (Fick's law). Two different physical situations have been studied: (i) vacancy-mediated hopping diffusion of atoms in a rigid face-centered-cubic lattice and (ii) continuous atom diffusion in a model liquid. In the former, the random walk of the vacancy-inducing atom diffusion is simulated, whereas, in the latter, continuous atom motion is studied via molecular dynamics. The results show that, in both systems, Fick's law is valid and, thus, the diffusion equation applies, even in the presence of the strongest possible tracer concentration gradients, provided that the diffusion time exceeds the value for the spreading of the tracer to become larger than a couple of nearest-neighbor distances. These findings are discussed and are compared with results available in the literature.

DOI: 10.1103/PhysRevB.85.144121 PACS number(s): 68.35.Fx, 66.30.Pa

I. INTRODUCTION

At the hydrodynamic limit, the motion of tracer particles in a matrix, viewed as a continuum, is satisfactorily described by the diffusion equation, governing the space and time evolution of the tracer distribution and flux. It allows the experimental determination of the diffusion tensor $\overline{\overline{D}}$, a thermodynamic quantity characteristic of the diffusion couple. However, there are several examples of experimental situations requiring that concentrations and fluxes of diffusing species are described at the atomic scale, such as nanoscopic devices in which long-lived large concentration gradients are desirable.[1,2] In such situations and/or under strong concentration gradients, Fick's law may not be applied,[3,4] and the diffusion equation should be replaced by a huge and possibly infinite set of coupled discrete equations, expressing mass conservation for tracer atoms, thus, increasing the complexity of the deconvolution of the experimental data. The validity of the diffusion equation in crystals at short diffusion times and in the presence of large concentration gradients has been studied by Martin and Benoist,[4] who have suggested that this equation may still be used providing that the wavelengths of the Fourier components of concentration profiles are much larger than the lattice parameter. However, no explicit thresholds for the concentration gradient or the diffusion time have been specified in this paper, and the proposed mathematical developments are inconsistent[3] (cf. Sec. V).

"Shall the diffusion equation apply at the atomic scale" is a question about the soundness of Fick's first law at this scale, empirically stating that fluxes of species and their concentration gradients are in linear relationships.[5] Besides the theoretical interest in establishing the domain of validity of this law, it is worthwhile investigating the matter in the nowadays context of the increasing importance of nanotechnologies. Indeed, during processing, the annealing of devices—such as quantum dot heterostructures in which atomistic strong composition gradients are customary—triggers the interdiffusion of species at the interfaces with the potential to alter their structural and optical properties.[6,7] Current modeling of composition-induced changes of the properties of such devices assumes that Fick's law may still be applied,[8] whereas, establishing the domain of validity of the diffusion equation at the atomic scale and in the presence of strong composition gradients would contribute to better defining the framework for modeling.

In the present paper, the validity of Fick's law at the atomic scale is tested by: (i) numerical simulations of vacancy-mediated self-diffusion in a rigid face-centered-cubic (fcc) lattice and (ii) a molecular-dynamics (MD) study of self-diffusion in a generic liquid modeled via the Lennard-Jones (LJ) (12-6) potential used for the sake of comparison. The results show that the diffusion equation can still be used at this scale provided that concentration gradients do not exceed a critical value and that the validity domain of this law extends far down in the atomic scale.

The following sections, Secs. II and III, respectively, are devoted to a brief overview of the theoretical background, to the methodology adopted in the present paper, serving the objective of a consistent representation of the results, and to the details about the models and the computations. The results are presented in Sec. IV. They are further commented on and are compared to those of papers in the literature[9,10] in Sec. V. This discussion section also includes conclusions and some perspectives.

II. THEORY AND METHODOLOGY

A. Theory

In a crystalline lattice, the local balance of diffusing tracer atoms leads to a near-infinite set of coupled equations,[3]

$$\frac{\partial c_i}{\partial t} = \frac{w}{2}\left(c_{i+1} + c_{i-1} - 2c_i\right). \tag{1}$$

Equation (1) can be rewritten in the following way:

$$\frac{\partial c_i}{\partial t} = -(j_{i+1/2} - j_{i-1/2}), \tag{2}$$

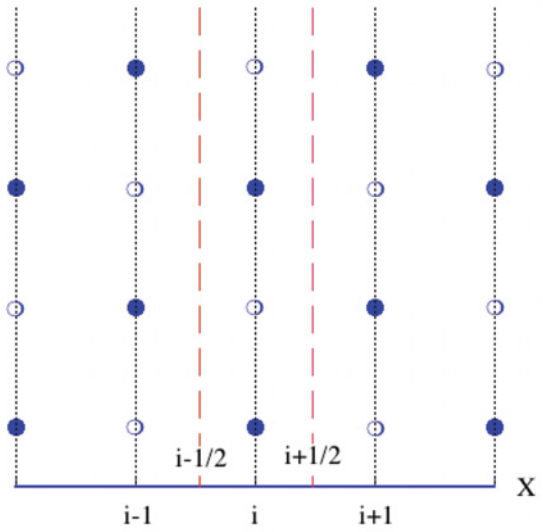

FIG. 1. (Color online) Schematic of atoms in (001) atomic planes of the face-centered-cubic lattice onto the figure plane (axis [001], stacking sequence: ABAB, . . .). Full and open symbols represent atoms in planes of type A or B, respectively.

where

$$j_{i+1/2} = \frac{w}{2}\,(c_i - c_{i+1})\,, \tag{3}$$

and

$$j_{i-1/2} = \frac{w}{2}\,(c_{i-1} - c_i)\,, \tag{4}$$

with c_i,$c_{i\pm1}$ representing the tracer concentrations expressed as atom percentages in adjacent atomic planes labeled i and $i \pm 1$, w is the atomic jump frequency, and $j_{i\pm1/2}$ are the net exchange fluxes of tracer atoms, evaluated at median positions between atomic planes (Fig. 1).

Assuming that a continuous and sufficiently derivable function $C(x,t)$ existed, such as $\forall\ i\ C(x_i,t) = c_i(t)$ and taking arbitrary values for $x \neq x_i$, Eq. (1) may be written[3]

$$\frac{\partial C(x_i,t)}{\partial t} = \frac{w}{2}\,[C(x_{i+1},t) + C(x_{i-1},t) - 2C(x_i,t)]\,, \tag{5}$$

and expanded in Taylor series, it becomes

$$\left.\frac{\partial C(x,t)}{\partial t}\right|_{x_i} = \frac{wd^2}{2}\left.\frac{\partial^2 C(x)}{\partial x^2}\right|_{x=x_i} + O(d^4), \tag{6}$$

with d as the jump distance. Providing that the terms of fourth order and above are neglected and the truncated equation is assumed holding at any abscissa, one finds the usual macroscopic diffusion equation with the diffusivity constant $D = wd^2/2$. Similarly, a continuous analog of the discrete equations (3) and (4) can be defined by means of a continuous flux function $J(x,t)$, such as[3]

$$J(x,t) = -\frac{wd}{2}\frac{\partial C(x,t)}{\partial x}. \tag{7}$$

Now, in the presence of strong concentration gradients,[4] the values of the discrete concentrations and fluxes, Eqs. (1)–(4), may significantly differ from those predicted by neglecting high-order terms and solving Eqs. (6) and (7). Assessing the magnitude of higher-order terms as a function of the concentration gradient requires high-accuracy measurements and, thus, experiments difficult to perform. Instead, the computer simulations of mass transport at the atomic scale employed in the present paper are better adapted for first addressing this question. The following section presents the adopted methodology.

B. Method

1. General approach

The method adopted in the present paper is the following:

(1) A simple case study is chosen: It represents self-diffusion in a one-component system of infinite extension in the three space directions in which a planar diffusion interface is created at initial time $t = 0$ by labeling A or B atoms with abscissas negative or positive, respectively. In this case, the thermodynamic force for mixing is the entropy of the configuration. This nonequilibrium method has been previously used by Kincaid in a paper aiming at calculating corrections to the hydrodynamic description of self-diffusion on short time scales.[9,10]

(2) At first, the considered case is a rigid fcc lattice. In such systems, self-diffusion is mainly vacancy mediated,[5] whereas, vacancy jumps of length equal to the first-neighbor distance are assumed. The numerical simulation consists of moving the vacancy at random and computing averages of the atomic mean-square displacements and of the species concentrations and fluxes (atoms A and B) on a plane-by-plane basis [Eqs. (1)–(4)]. To ensure that statistical averages of these quantities are meaningful, the number of vacancy jumps is chosen large enough for the numerical values of the atomic correlation factor to converge toward the theoretical value with accuracy better than 1%.

(3) Simulation results can then be compared to the values predicted by the analytic solution of the diffusion equation, corresponding to these specific initial and boundary conditions on a plane-by-plane basis. The comparison is, however, a painful task since the diffusion profiles extend over an increasingly large number of atomic planes as the number of vacancy jumps increases. Fitting the analytical solutions of the diffusion equation to the numerical values of the concentration and the fluxes circumvents this difficulty. Thus, one obtains two estimates of the Dt value, where D is the self-diffusivity and t is the "annealing" duration to be compared to the theoretical prediction of atom diffusion in the bulk, driven by the random walk of thermal equilibrium vacancies. Differences between these estimations and the bulk diffusivity are attributed to the diffusion equation failing to apply at the atomic scale. They are visualized via the graphical representations of concentrations and fluxes on a plane-by-plane basis (cf. Sec. IV).

(4) Molecular-dynamics simulations of self-diffusion in a model liquid provide additional information about the applicability of the diffusion equation in a position-disordered system in which mass transport proceeds via continuous atom movements. The investigation proceeds in the same way as for the rigid-lattice case [see point (3)], except that instead of computing the Dt products, diffusivity values are obtained as the time variable is here explicitly known.

2. Application details

Solving the macroscopic one-dimensional diffusion equation for an initial step distribution of a tracer ($t = 0$, $C = 1$ if $x \geqslant 0$ and $C = 0$ otherwise) leads to the following expressions for the tracer concentration $C(x,t)$ and flux $J(x,t)$ as functions of the position and time (constant source diffusion problem),[5]

$$C(x,t) = \frac{1}{2}\left[1 + \mathrm{erf}\left(\frac{x}{2\sqrt{Dt}}\right)\right], \tag{8}$$

$$J(x,t) = -D\frac{\exp\left(-\frac{x^2}{4Dt}\right)}{4\sqrt{\pi\, Dt}}. \tag{9}$$

For both systems studied in this paper, the simulations provide numerical values of the concentration and the flux of the species, respectively, $c_k(x_i,t)$ and $j_k(x_i,t)$ (k = A,B) on a plane-by-plane basis. Adjusting Eqs. (8) and (9) to these data provides, in general, two different values of the quadratic tracer spreading $2D_c t$ and $2D_j t$, respectively, where t is the annealing time. In the limit of weak concentration gradients or long annealing times, $D_c = D_j = D_b$ is expected to hold, where D_b denotes the bulk diffusivity evaluated in both systems via the Einstein or the Green-Kubo relations.[5] Otherwise, the values should be different $D_b \neq D_c \neq D_j \neq D_b$.[3]

III. MODELS AND COMPUTATIONS

In the present paper, a close equivalence is guaranteed between the "constant source" diffusion problem and the size-limited computational models by verifying that, for all the computations presented below, a bulk region is preserved in subsystems A or B.

A. Rigid lattice

Three fcc lattice models have been used with linear dimensions along the $X\|[100]$, $Y\|[010]$, and $Z\|[001]$ space directions, corresponding to $30 \times 5 \times 5$, $30 \times 10 \times 10$, $30 \times 20 \times 20$, and $30 \times 30 \times 30$ Bravais lattice cells. The origin of the coordinates is positioned at the mass center of the computational boxes, and a vacancy is created at a lattice site chosen at random. Vacancy diffusion is simulated by exchanging the defect with one of its 12 first neighbors, chosen with equal probability, whereas, surface effects have been circumvented by using periodic boundary conditions within the minimum image convention. This process is repeated up to 10^6 times for 10^3 initial configurations differing from each other by the different initial position of the vacancy. The squared displacements of atoms are averaged over all the initial configurations and are recorded as a function of the number of vacancy jumps. These computations allow for the estimation of the atomic correlation factor f for the vacancy diffusion in the fcc lattice,

$$f = \frac{\langle \delta r_i^2 \rangle_N}{n_v d_{1nn}^2}, \tag{10}$$

and of the discrete values of the concentration of the species c_l^k in the atomic planes l, where n_v is the number of vacancy jumps, N is the number of atoms in the model, d_{1nn} is the jump length, set equal to the first-neighbor distance, and brackets $\langle\,\rangle_N$ denote averages of squared atomic displacements over all the atoms i in the model. However, atomic fluxes, $j_{i\pm1/2}^k$ [Eqs. (3) and (4), k = A,B) cannot be determined without the knowledge of the atomic jump frequency w, a value that is not specified within the rigid-lattice model. This is why, throughout this paper, computed flux values are expressed in units reduced by the atomic jump frequency $J^{\#} = J/w$, whereas, the bulk atomic diffusion coefficient D_b is replaced by

$$D_b \delta t = \frac{1}{6} f \frac{n_v}{N} d_{1nn}^2, \tag{11}$$

where δt is the annealing duration. Given the method adopted in this paper, testing the diffusion equation for applicability at the atomic scale requires that the numerical estimation of the atomic correlation factor has converged with reasonable accuracy to its theoretical value $f = 0.781\,45, \ldots,$[11] for the vacancy mechanism.

B. Lennard-Jones liquid

A Lennard-Jones (12-6) system has been simulated by using molecular dynamics with potential parameters: $\sigma = 0.3405$ nm and $\varepsilon = 119.8$ K, adapted for argon,[12] at reduced density $\rho^* = \rho\sigma^3 = 0.85$ and temperature $T^*/(\varepsilon/k_B) = 1.67$, where k_B is the Boltzmann constant. The chosen thermodynamic state point is well within the region of stability of the liquid according to the phase diagram of the Lennard-Jones (12-6) potential found in the literature.[12] For the sake of comparison with the rigid fcc lattice, the system was made of $N = 12\,000$ point particles, contained in a computational box with periodic boundary conditions acting along the X, Y, and Z directions and with linear dimensions $30 \times 10 \times 10 \times (1.6755\sigma)$.[3] Interactions were cut off at a distance of $r_c = 2.5\sigma$. The Newtonian equations of motion were integrated with a time step $\Delta t_{MD} = 4.64 \times 10^{-4}(m\sigma^2/\varepsilon)^{1/2}$where m is the atomic mass. Reduced Lennard-Jones units are used throughout the text. The liquid state has been obtained from an initially crystalline configuration equilibrated for a time long enough to ensure that the specific heat has reached a stationary value. Like the rigid-lattice case, the computational box has been divided along the X axis in two equal volume subsystems in which atoms were labeled A or B, respectively. Starting from a well-equilibrated configuration, an equilibrium trajectory made of $n = 10^7$ time steps has been produced, and average distribution profiles and fluxes of atoms A and B have been computed as a function of the annealing time.

Expressing mass conservation in a crystal, as in Sec. II A, relies explicitly on the lattice geometry. Thus, the question arises how the procedure presented in Sec. II B should be reformulated in a liquid since, in this case, the average mass density is a continuous and uniform function of the position. For this purpose, the computational box has been divided in $n_l = 1024$ sublayers of equal thickness along the X axis, a good compromise between the needs of a fine resolution of the composition and flux profiles and that of reducing the statistical noise to an acceptable level since the latter is directly related to the particle content of the sublayers. Moreover, the equilibrium MD trajectory is broken in segments of length t,

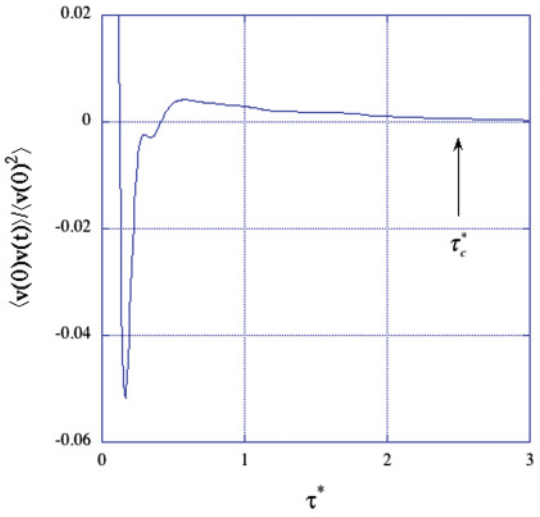

FIG. 2. (Color online) Lennard-Jones liquid: normalized velocity self-correlation function at reduced density $\rho^* = 0.85$ and temperature $T^* = 1.67$. Molecular correlations are seen to vanish for time delays longer than $\tau_c^* \approx 2.5$.

the first configuration in each segment serving as an initial state. The frontier between species A and B is located at the abscissa $X = 0$. "Sliding" averages of distributions and fluxes are then computed over the equilibrium trajectory,

$$c_l^k(x,t) = \frac{1}{V_l}\left\langle \sum_{i=1}^{n_l} \delta\left(x - x_{i,l}^k\right)\right\rangle_t , \tag{12}$$

$$j_l^k(x,t) = \frac{1}{V_l}\left\langle \sum_{i=1}^{n_l} v_{i,l}^{x,k}\,\delta\left(x - x_{i,l}^k\right)\right\rangle_t , \tag{13}$$

where k (k = A,B), denotes the atom species and $c_l^k(x,t)$, n_l, $v_{i,l}^{x,k}$, and V_l, respectively, represent the k-atom concentration, the number of particles, the x component of the k-atom velocity in layer l, and the volume of the sublayers. The brackets indicate sliding averages over segments of length t, composing the MD trajectory.

For the reference purpose, the self-diffusion coefficient of the bulk liquid has been calculated via the Green-Kubo relation,

$$D = \frac{1}{3}\int_0^\infty \langle \vec{v}(\tau)\vec{v}(0)\rangle\, d\tau . \tag{14}$$

Figure 2 displays the velocity autocorrelation as a function of the delay τ, the numerical integration of which yields the bulk diffusivity in the liquid at this state point $D^* = 0.1032$. This value is in satisfactory agreement with the prediction $D^*_{\mathrm{LV}} = 0.0918$, made using an interpolation formula introduced by Levesque and Verlet,[13] which reproduces the self-diffusion coefficient of the Lennard-Jones liquid as a function of the density and the temperature.

C. Least-squares fits

Equations (8) and (9) have been adjusted to the numerical profiles of compositions and fluxes by using the least-squares method and the multidimensional minimization package MERLIN.[14]

IV. RESULTS

A. Diffusive motion: Time scales

1. Crystals

Atom diffusion in crystals is a correlated walk, for it is mediated by the random motion of point defects present at very low concentrations, even at the melting temperature. In fcc crystals, self-diffusion is mainly due to the random movement of thermal vacancies, whereas, the departure from randomness of the atomic motion enters the microscopic definition of the atom diffusivity via the correlation factor f_v.[5,11] From the simulations, an estimation of its value is obtained via Eq. (10) by computing the atomic mean-square displacement (MSD) and extrapolating the value in the long-time limit. Figure 3(a) shows that the relative error committed in estimating f_v rapidly reaches a system-size-dependent "plateau" for MSDs larger than $\langle \delta r^2\rangle/a^2 \approx 10$, where a is the Bravais lattice constant.

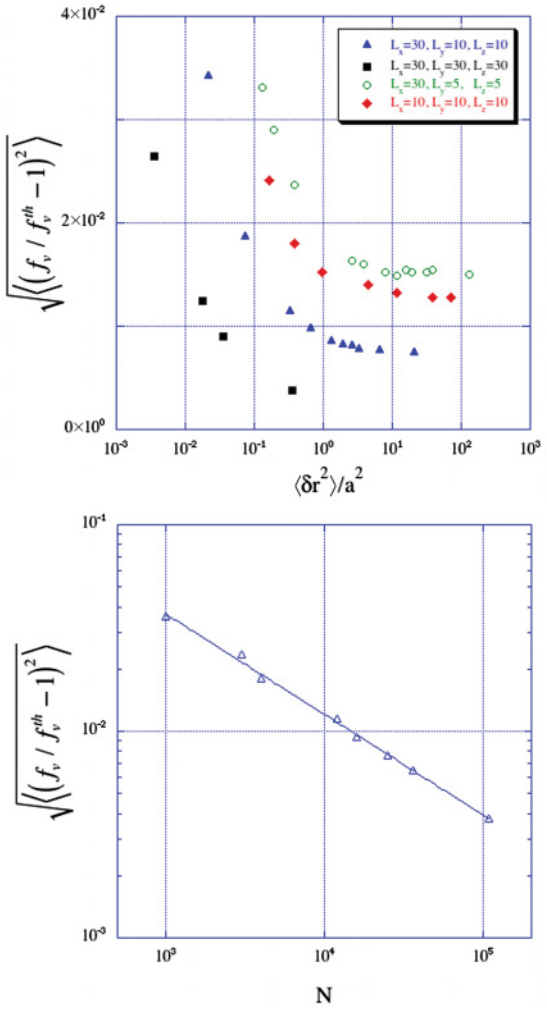

FIG. 3. (Color online) Vacancy diffusion on a fcc rigid lattice. Relative deviation of the numerical estimation of the atomic correlation factor from its theoretical value: (a) as a function of the atomic mean-square displacement for different system sizes (Lx,Ly,Lz): open circles, (30,5,5); diamonds, (10,10,10); triangles, (30,10,10); and squares, (30,30,30) and (b) as a function of the number of atoms N at a fixed value of the atomic mean-square displacement $\langle \delta r^2\rangle/a^2 = 0.39$ (a, Bravais lattice constant).

Figure 3(b) shows that, at any fixed value of the atomic MSD, here $\langle \delta r^2 \rangle / a^2 \approx 0.39$, the relative error committed on f_v with respect to the theoretical value [$f_v^{th} = 0.781\,45, \ldots$ (Refs. 15 and 16)] decreases when the system size increases. Most of the results presented below were obtained with a system made of $30 \times 10 \times 10$ Bravais lattice cells ($N = 12\,000$ atoms), resulting in a relative error committed on f_v, lower than 10^{-2}. This compromise minimizes the computational effort though preserving sufficient accuracy in estimating f_v and, thus, the bulk diffusivity. Moreover, Fig. 3(a) shows that f_v reaches a system-size-dependent plateau at large MSDs with values representing the best possible estimation of this quantity for any given system size. This is the direct consequence of the cutoff imposed by the boundary conditions on the diffusion paths of the vacancy and the atoms.

2. *Liquids*

Like diffusion in crystalline solids, atomic MSDs in liquids do not reach the asymptotic linear variation with elapsed time (Einstein equation) before the effective decay of the particle velocity self-correlation function (Fig. 2). In the context of the present paper, species distributions and fluxes in the liquid phase have been computed for diffusion times always higher than $\tau_c^* > 2.5$, the characteristic time for velocity correlations to vanish (Fig. 2).

B. Self-diffusion in the fcc rigid lattice

Vacancy-mediated self-diffusion has been investigated as described in the above Secs. II B and III A. Figure 4(a) represents the distribution of species B as a function of the reduced abscissa X/a (a, the Bravais lattice constant) for different annealing times. The spreading of B atoms at the interface, after annealing during a time interval δt, is characterized by the quantity $\delta X_c = 2\sqrt{D_c \delta t}$ and is obtained from a least-squares adjustment of Eq. (8) to the simulation data. The figure shows that Eq. (8), plotted with these values, fits the tracer concentration profiles nicely (full, dashed, and dotted lines). Once concentrations of species B are known, the corresponding flux values are obtained as a function of the atomic plane positions from Eqs. (3) and (4). Adjusting Eq. (9) on these data yields another set of $\delta X_j = 2\sqrt{D_j \delta t}$ that accurately reproduces the corresponding discrete flux values [full lines in Fig. 4(b)]. If the diffusion equation is valid at the atomic scale, the relation $\delta X_c = \delta X_j$ should always hold. Figure 4(b) shows that this is generally true except for the shortest annealing duration (triangles) for which the graphs of Eq. (9) with δX_c (dashed lines) or δX_j values (full lines) reveal significantly different. This finding suggests that the failure of the diffusion equation at the atomic scale can be efficiently monitored by plotting the ratios D_c/D_b and D_j/D_b as a function of $\sqrt{2D_i \delta t}$, where $D_i = D_c, D_j$ and D_b is the bulk diffusivity computed as indicated in Sec. III A. Figure 5 represents these ratios as a function of $X = \sqrt{2D_i \delta t}/a$ (a, the Bravais lattice constant). For $X > X_{cr} \approx 2.5$, both ratios have practically converged to value one, establishing thereby that above this critical diffusion length, the continuous diffusion equation can be safely used.

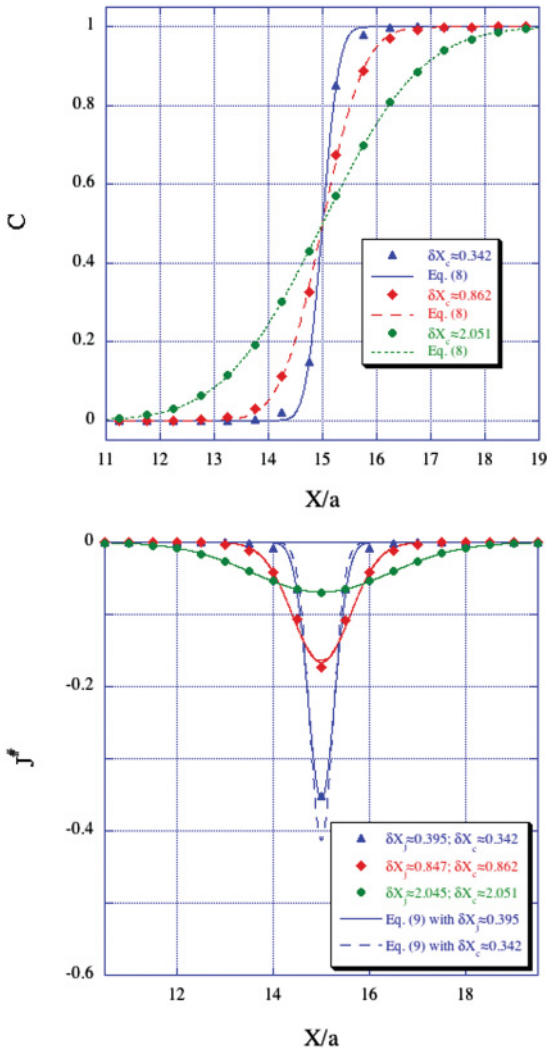

FIG. 4. (Color online) Rigid lattice: (a) atomic concentration of B atoms as a function of the positions of the (100) atomic planes expressed in units of the Bravais lattice constant a. Full lines represent the graphs of Eq. (8) using values of $\delta X_c = 2\sqrt{D_c \delta t}$: triangles, $\delta X_c \approx 0.342$; diamonds, $\delta X_c \approx 0.862$; full circles, $\delta X_c \approx 2.051$. (b) Fluxes of B atoms in reduced units (see Sec. III A) corresponding to the concentration profiles displayed in (a). Full lines: graphs of Eq. (9) with δX_j values, triangles, 0.395; diamonds, 0.847; and full circles, 2.045. Dashed lines: graphs of Eq. (9) with δX_c values obtained from adjustments of Eq. (8) to the concentration profiles [see (a)]. In this figure, full and dashed lines are distinct only for the data series corresponding to the shortest annealing time (triangles).

C. Self-diffusion in the Lennard-Jones liquid

In the Lennard-Jones liquid, average profiles of concentration and flux of B atoms were computed as a function of elapsed time δt over an equilibrium MD trajectory of 10^7 time steps [Eqs. (12) and (13)].

Figure 6(a) displays the concentration profiles of B-atom species as a function of the position at reduced elapsed times $\delta t_1^* = 2.5$ and $\delta t_2^* = 26.1$ together with the least-squares fit of Eq. (8) to the MD data. The time needed for molecular correlations to vanish (Sec. IV A) is δt_1^*, whereas, δt_2^* is a time value chosen arbitrarily as a representative of long annealing

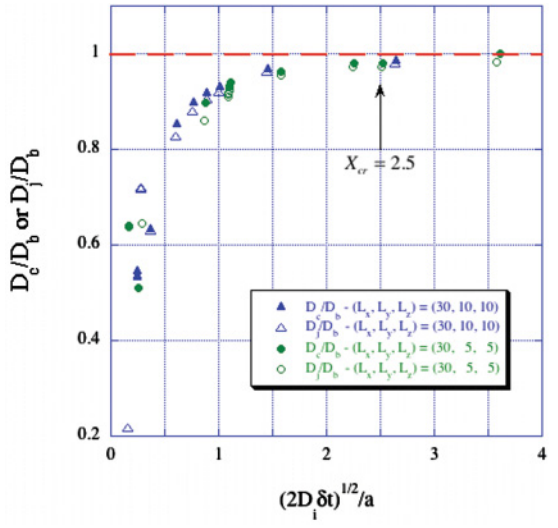

FIG. 5. (Color online) Rigid lattice: full symbols, diffusivity ratios D_c/D_b and open symbols, D_j/D_b, where D_b is the bulk diffusivity as a function of $X = (2D_i\delta t)^{1/2}/a$ ($i = c, j$; a, the Bravais lattice constant). Triangles: system size $30 \times 10 \times 10$ lattice cells, circles: system size $30 \times 5 \times 5$ lattice cells.

durations. The corresponding diffusivity values $D^*_{c,1} = 0.097$ and $D^*_{c,2} = 0.0985$ are very close to the value of the bulk diffusivity obtained via the Green-Kubo integral (Sec. II B) $D^*_b = 0.1032$. It is worth noting that the MD data at the diffusion interface ($X^* = 25$) cope with the prediction of the macroscopic diffusion equation $C_{X^*=25} = 0.5$ at any time.

For the sake of clarity, the flux profiles are presented separately in Figs. 6(b) and 6(c) at δt^*_1 and δt^*_2, respectively, together with the fits of Eq. (9) to the MD data (full lines). Dotted lines in these figures represent the graphs of Eq. (9) using $\delta X = 2\sqrt{D_c\delta t}$ values extracted from the above fits of Eq. (8) on the concentration profiles [Fig. 6(a)]. Full and dotted lines are difficult to distinguish from each other, especially in Fig. 6(c), thus, indicating that D^*_c and D^*_j have practically converged to a common value.

Similar to Fig. 5, Fig. 7 represents the diffusivities D^*_c or D^*_j in the LJ liquid as a function of the average diffusion distance of B atoms at the interface $X^*_i = \sqrt{2D^*_i\delta t^*}(i = c, j)$. It appears that both diffusivity estimations have converged to the bulk diffusivity value D^*_b (dashed horizontal line) for average diffusion distances larger than a critical value $X^*_{cr} \approx 1.75$. Unlike D^*_c, D^*_j has practically converged to D^*_b for diffusion lengths larger than $X^*_{vmc} = \sqrt{2D_j\tau_c} \approx 0.70$, where $\tau^*_c \approx 2.5$ is the critical delay for molecular correlations to vanish. Moreover, the time delay $\delta t^* \approx 16$ for reaching the critical diffusion distance X^*_{cr} largely exceeds τ^*_c, meaning that the molecular correlations cannot be invoked to explain the failure of the continuous diffusion equation in the diffusion time interval [0.7,1.75].

V. DISCUSSION AND CONCLUSIONS

The results of this paper are of practical importance for all the situations requiring that mass transport be described at the atomic scale, some of which are listed and are commented on in Ref. 4, namely, relaxation or resonance methods for

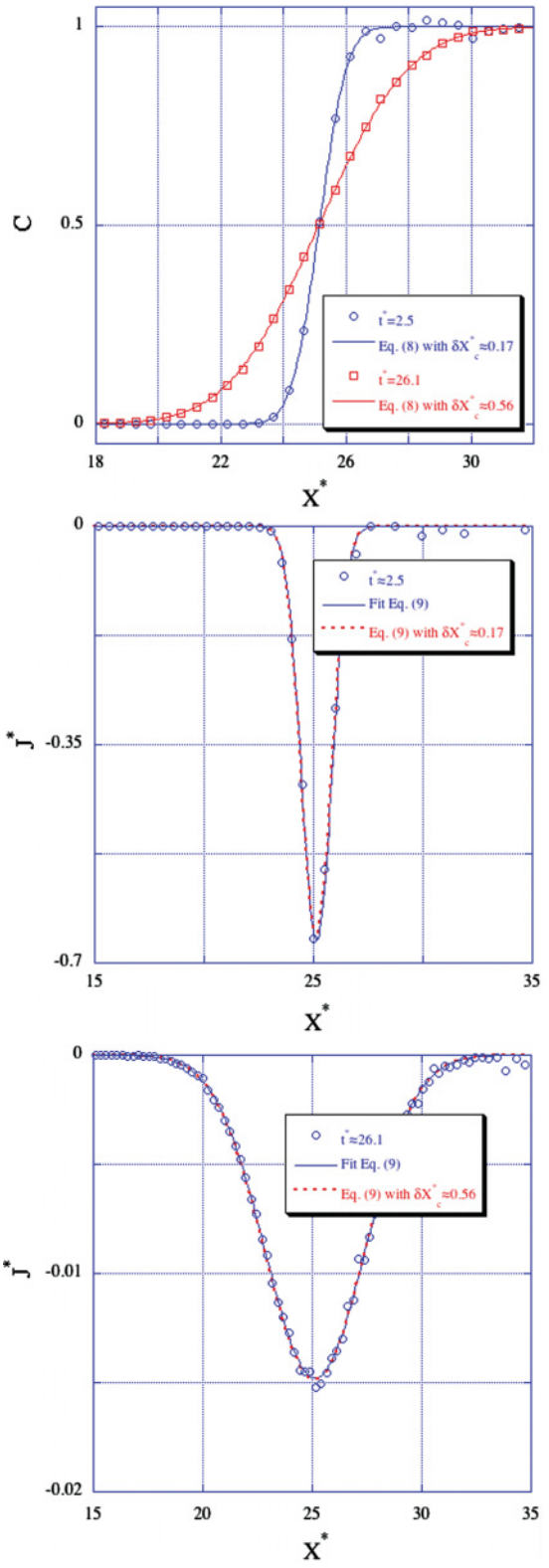

FIG. 6. (Color online) Lennard-Jones liquid: (a) Atomic concentration of B atoms as a function of the position at elapsed times open circles, $\delta t^*_1 = 2.5$ and open squares, $\delta t^*_1 = 26.1$. Full and dashed lines represent the fits of Eq. (8) to the MD data. (b) Flux of B atoms as a function of the position at elapsed time $\delta t^*_1 = 2.5$. Full line: Eq. (9) fitted to the MD data, dotted line: Eq. (9) with $\delta X^*_c = 0.17$ deduced from the fit of Eq. (8) to the concentration profile (a). (c) Same as in (b) at reduced elapsed time $\delta t^*_2 = 26.1$ and $\delta X^*_c = 0.56$.

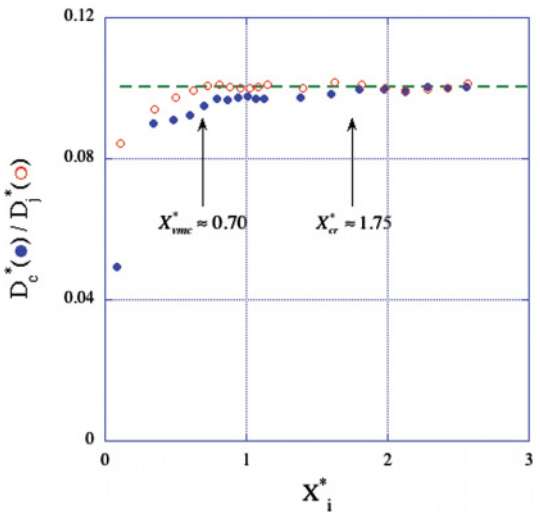

FIG. 7. (Color online) Lennard-Jones liquid: diffusivity values as a function of the spreading of tracer atoms (B atoms) at the diffusion interface $X_i^* = (2D_i^*\delta t^*)^{1/2}$. The values reported, D_c^* and D_j^*, are determined from least-squares fits of Eqs. (8) and (9) on the MD profiles of concentrations and fluxes. The horizontal dashed line marks the value of the converged bulk diffusivity D_b computed via the Green-Kubo integral of the self-correlation function of particle velocities. D_c and D_j have nearly converged to the bulk diffusivity value for values of the tracer spreading larger than $X^*_{\text{critical}} \approx 1.75$, whereas, the value $X^*_{vmc} \approx 0.7$ represents the diffusion length at vanishing molecular correlations.

studying atomic jumps, studies of the kinetics of clustering and nucleation of ordered phases, diffusion at grain boundaries, and surface diffusion under irradiation. One should also add to this nonexhaustive list, the problem of modeling the properties of nanostructured devices, which are tightly related to metastable compositions and atomistic strong composition gradients. The results obtained in this paper (Sec. IV) show that the condition $D_c = D_j = D_b$ is verified only above a threshold value of the tracer spreading, whereas, for short annealing durations, the values found are all different $D_b \neq D_c \neq D_j \neq D_b$ with D_c,D_j underestimating the bulk diffusivity systematically. Moreover, these conclusions hold whatever is the atomic structure of the system, crystalline or disordered (liquid).

Although the above-listed physical situations of interest are more complicated than the simple case of self-diffusion in crystals and liquids, the present paper establishes a method for deciding on whether or not the diffusion equation can safely replace the mass-conservation equations (1)–(4) by showing how an estimate can be determined for the critical annealing time or, equivalently, for the critical diffusion length above which higher-order terms, appearing in Eq. (6), are negligible. Moreover, the statement made in Ref. 4, that the diffusion equation does not hold for high-concentration gradients and/or short diffusion times should be weakened as the findings of the present paper show that the diffusion equation still correctly describes mass transport at the atomic scale for very-short diffusion times and considerably large concentration gradients.

The validity of this generic conclusion is likely to extend over systems with mass transport mediated by mechanisms other than vacancy diffusion. This suggestion is supported by the close similarities, revealed in the present paper, existing between crystals and liquids. However, additional work is certainly required before extending the validity of this conclusion to chemical diffusion in heterostructures or self-diffusion in grain boundaries, for these are more complex cases than the ones investigated here because of the dependence of the diffusivity on the concentration of the species in the former and the multiplicity of operating diffusion mechanisms in the latter.[17,18]

Since Martin and Benoist[4] have proposed analytic arguments for discussing the atomic scale validity of the diffusion equation at short times and large concentration gradients, it was tempting to compare their results to the findings of our present paper. However, their arguments rely on a Taylor series expansion of the discrete concentrations c_i, entering Eq. (1), a mathematically incorrect procedure since the derivative of the discrete function $c_i(x)$ does not exist. Accordingly, the comparison is not possible between the predictions of the aforementioned paper and the results of the present numerical simulations.

In Sec. II B, it was already mentioned that the nonequilibrium method used in the present paper was already employed by Kincaid, who used MD simulations and a Lennard-Jones liquid for testing the validity of analytical corrections for the hydrodynamic description of self-diffusion on short time scales and the applicability of the telegrapher's equation for mass transport.[9,10] In relation with the present calculations, these papers suggest that, in liquids, "...the diffusion equation solution spreads too rapidly," a conclusion drawn by comparing MD calculations of the spreading of an initially thin film of labeled atoms with the analytical solution of the diffusion equation. This conclusion is not confirmed by the present paper, which shows instead that differences between the discrete description of mass flow and its continuous counterpart, i.e., the analytical solution of the diffusion equation exist only for tracer profiles extending over less than a couple of interatomic distances. Moreover, in his MD calculations, Kincaid[10] computed a tracer distribution at times so short that molecular correlations were still very strong, whereas, he used the converged (long-time) diffusivity in the bulk liquid $D^* = 0.412$ for solving the diffusion equation at these time values.[19] Figure 8(a) displays the velocity autocorrelation function of a Lennard-Jones liquid made of $N = 4000$ point particles at the state point $T^* = 2.0$, $\rho^* = 0.5$, also studied by Kincaid. In this figure, arrows mark the time delays used by Kincaid and the values of the Kubo integral computed up to this time. It visualizes how molecular correlations affect the value of the diffusivity in the bulk liquid. In the present paper, the liquid was simulated over time intervals longer than the characteristic correlation time $\tau_c^* \approx 2.5$ (Fig. 2) at the studied state point, whereas, in the fcc crystal, the simulated vacancy trajectories were systematically longer than the minimum length required for the atomic correlation factor to converge satisfactorily. Consequently, the reported results all satisfy the requirement that the diffusivity in the bulk of the studied systems has practically converged to its value at the thermodynamic limit.

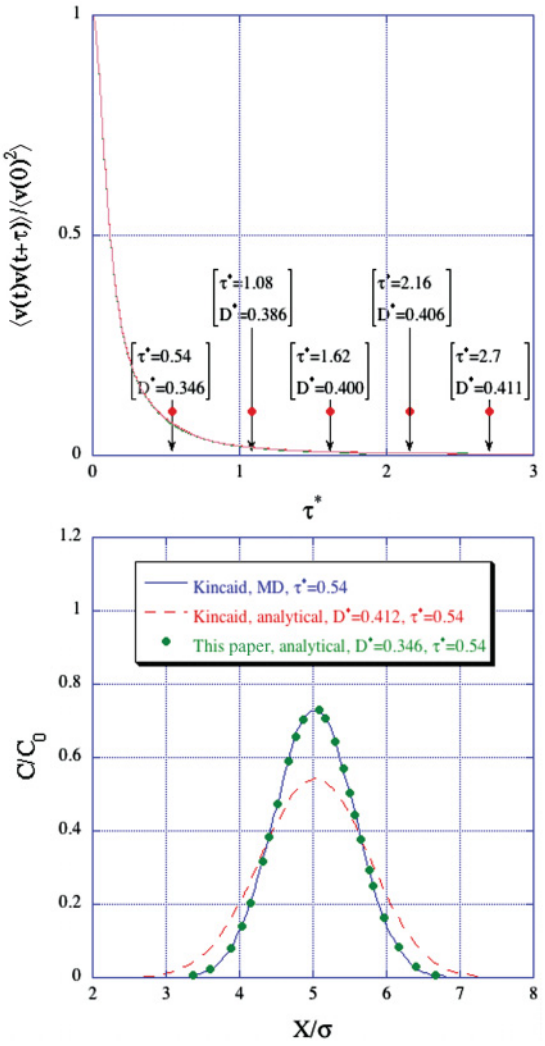

FIG. 8. (Color online) (a) Equilibriumvelocity autocorrelation function in a Lennard-Jones liquid at the state point $T^* = 2.0$, $\rho^* = 0.5$, and its Kubo integral values (diffusivity) at the delays used in Kincaid's paper.[10] At elapsed time values shorter than $\tau^* = 2.7$, molecular correlations are still significant. (b) Full line: shape of an initial thin-film distribution of a tracer in a Lennard-Jones liquid at the state point $T^* = 2.0$, $\rho^* = 0.5$ after annealing during $\tau^* = 0.54$, redrawn from Kincaid's MD paper.[10] Full circles: the thin-film solution of the diffusion equation using the diffusivity value $D^* = 0.346$ [see (a)], dashed line: the thin-film solution of the diffusion equation using the diffusivity value $D^* = 0.412$ as performed in Ref. 10.

In disagreement with the conclusion drawn by Kincaid, Fig. 8(b) shows that the thin-film solution of the diffusion equation at time $\tau^* = 0.54$ and diffusivity value $D^* = 0.346$ [Fig. 8(a), full circles] fits his MD results redrawn in this figure (full line) perfectly. For the comparison purpose, the thin-film solution he has used at this time with $D^* = 0.412$ is also displayed in this figure (dashed line).

The present paper shows that, in the absence of molecular correlations, separate fits of the solutions of the diffusion equation on the MD concentration and flux profiles yield diffusivity values that significantly underestimate the converged bulk diffusivity for diffusion distances shorter than $X^*_{cr} \approx 1.75$. This is the atomic scale effect Ghez[3] explains on phenomenological grounds.

A mathematical analog of Fick's equation is the Fourier law, describing the evolution of thermal energy as a function of the temperature gradient. Like the diffusion case, the validity of this equation at the atomic scale has been a matter of discussion until Ciccotti and Tenebaum[20] addressed this problem. These authors used MD and a Lennard-Jones (12-6) model of argon to study heat transfer under strong temperature gradients at the atomic scale. Similar to the findings of the present paper, their results show that Fourier's law is still valid under remarkably strong temperature gradients, whereas, the thermal conductivity obtained from these calculations compares favorably with experimental data for argon.

In conclusion, in this paper, we have shown that the diffusion equation applies at the atomic scale whenever the diffusion distances are longer than a couple of first-neighbor distances whatever is the atomic structure of the considered system, crystalline or disordered (liquid). Work in progress focuses on the validity of the diffusion equation in model heterostructures in connection with the prediction of the properties of nanostructured devices.

ACKNOWLEDGMENTS

This work has been motivated by discussions which lasted over recent years between one of the authors (V.P.) and students of the masters degree "Matériaux pour les Structures et l'Energie (MSE)" at the "Institut des Sciences et Techniques Nucléaires (INSTN)" of the "Commissariat à l'Energie Atomique et Les Energies Alternatives (CEA)." The constant support of Dr. C. Meis, in charge of the educational program at INSTN, is warmly acknowledged. The authors also thank Professor E. Hicks, Professor J. Kioseoglou, and Professor T. Karakostas for critical reading of the manuscript.

*Corresponding author: Vassilis.Pontikis@cea.fr

[1] H. C. Torrey, Phys. Rev. **92**, 962 (1953).
[2] J. E. Hook and J. E. Hilliard, J. Appl. Phys. **40**, 2191 (1969).
[3] R. Ghez, *Diffusion Phenomena: Cases and Studies*, 2nd ed. (Kluwer Academic/Plenum, New York, 2001).
[4] G. Martin and P. Benoist, Scr. Metall. **11**, 503 (1977).
[5] J. Philibert, *Atom Movements: Diffusion and Mass Transport in Solids* (Les Editions de Physique, Les Ulis, France, 1991).
[6] S. Magalhaes, K. Lorenz, N. Franco, N. P. Barradas, E. Alves, T. Monteiro, B. Amstatt, V. Fellmann, and B. Daudin, Surf. Interface Anal. **42**, 1552 (2010).
[7] D. Fuhrman, H. Jönen, L. Hoffmann, H. Bremers, U. Rossow, and A. Hangleiter, Phys. Status Solidi C **5**, 1662 (2008).
[8] C. C. Chen, T. H. Hsueh, Y. S. Ting, G. C. Chi, and C. A. Chang, J. Appl. Phys. **90**, 5180 (2001).
[9] J. M. Kincaid, Phys. Rev. Lett. **74**, 2985 (1995).

[10]J. M. Kincaid, Fluid Phase Equilib. **150-151**, 133 (1998).
[11]A. R. Alnatt and A. B. Lidiard, Rep. Prog. Phys. **50**, 373 (1987).
[12]J.-P. Hansen and L. Verlet, Phys. Rev. **184**, 151 (1969).
[13]D. Levesque and L. Verlet, Phys. Rev. A **2**, 2514 (1970).
[14]D. G. Papageorgiou, I. N. Demetropoulos, and I. E. Lagaris, Comput. Phys. Commun. **159**, 70 (2004) (computer program available at [http://www.sciencedirect.com/science/journal/00104655]).
[15]J. L. Bocquet, G. Brebec, and Y. Limoge, in *Physical Metallurgy*, edited by R. Cahn and P. Haasen (North-Holland, London, 1996), p. 535.
[16]D. K. Chaturvedi and A. R. Allnatt, Philos. Mag. A **69**, 821 (1994).
[17]M. Guillopé, G. Ciccotti, and V. Pontikis, Surf. Sci. **144**, 67 (1984).
[18]T. Kwok, P. Ho, and S. Yip, Phys. Rev. B **29**, 5363 (1984).
[19]J. M. Kincaid, R.-F. Tuo, and M. Lopez de Haro, Mol. Phys. **81**, 837 (1994).
[20]G. Ciccotti and A. Tenenbaum, J. Stat. Phys. **23**, 767 (1980).